CHEMISTRY OF MATERIALS
Article

Chem. Mater. **2009,** *21,* 5491–5498 5491
DOI:10.1021/cm902502c

Versatile Catalytic System for the Large-Scale and Controlled Synthesis of Single-Wall, Double-Wall, Multi-Wall, and Graphene Carbon Nanostructures

Enkeleda Dervishi,*[,†] Zhongrui Li,[†] Fumiya Watanabe,[†] Aurelie Courte,[‡] Abhijit Biswas,[§] Alexandru R. Biris,[⊥] Viney Saini,[†] Yang Xu,[†] and Alexandru S. Biris*[,†]

[†]*Nanotechnology Center, University of Arkansas at Little Rock, Arkansas 72204,* [‡]*Ecole d'Ingénieurs du CESI-EIA, 86 Route de Breuty, Domaine Universitaire, 16400 La Couronne, France,* [§]*Department of Physics, University of Oklahoma, Norman, Oklahoma 73019, and* [⊥]*National Institute for Research and Development of Isotopic and Molecular Technologies, P.O. Box 700, R-400293 Cluj-Napoca, Romania*

Received August 14, 2009. Revised Manuscript Received October 6, 2009

This work reports a low-cost production method of carbon nanotubes (CNTs) and few-layer graphene sheets in large quantities through radio-frequency catalytic chemical vapor deposition (RF-cCVD). As the reaction temperature was varied over a range of 700−1000 °C, different types of high-quality carbon nanostructures were synthesized on a single Fe−Co/MgO catalytic system, while utilizing acetylene as the hydrocarbon source. The reaction efficiencies were found to be dependent on the morphological properties of the corresponding nanostructures and varied significantly with the synthesis temperature. Highly crystalline multi-wall, double-wall, and single-wall CNTs were obtained when the temperature was in the range of 700−950 °C, whereas large quantities of few-layer graphene sheets (1−5 layers) were synthesized at 1000 °C. The carbon nanostructures were characterized via several analytical techniques, such as electronic microscopy, Raman spectroscopy, X-ray diffraction, etc. It was determined that the synthesis temperature had a strong influence, both on the catalyst system and on the type of the nanostructures synthesized. By utilizing the same catalytic system and varying only one reaction parameter, it may be possible to reduce the production cost of CNTs and graphene nanosheets significantly, so that they may be utilized in various advanced applications.

Introduction

Since the discovery of CNTs, a vast amount of research has been done to fully understand the mechanism and kinetics of nanotube formation.[1] CNTs have exceptional properties that make them attractive for numerous applications such as nanoelectronics, energy storage, chemical sensors, and other recently discovered nano-applications.[2−7] Synthesis conditions such as catalyst composition, reaction temperature, hydrocarbon type, and flow rates of the carrier and hydrocarbon gas have enormous influences on nanotube growth.[8−10] Utilizing a chemical vapor deposition (CVD) method, the morphological properties of CNTs can be controlled to a certain extent by varying the reaction parameters.[11] This method of production is very versatile and has also been utilized to synthesize graphene in large quantities.[12]

Graphene is comprised of a single-layer of sp^2-hybridized C atoms, hexagonally arranged into a two-dimensional array. Because of its unique physical, chemical, electrical, and mechanical properties, this material has shown promise for several advanced technological applications such as graphene-based composite materials, fuel cells, batteries, chemical detectors, solar cells, nanoelectronics, and photovoltaic devices.[13−18] The production of large-scale and high-quality graphene via a simple

*Authors to whom correspondence should be addressed. E-mails: exdervishi@ualr.edu (E.D.), asbiris@ualr.edu (A.S.B.).

(1) Iijima, S. *Nature* **1991**, *354*, 6348.
(2) Li, Z.; Kandel, H. R.; Dervishi, E.; Saini, V.; Xu, Y.; Biris, A. R.; Lupu, D.; Salamo, G. J.; Biris, A. S. *Langmuir* **2008**, *24*, 2655.
(3) Kumashiro, R.; Hiroshiba, N.; Komatsu, N.; Akasaka, T.; Maeda, Y.; Suzuki, S.; Achiba, Y.; Hatakeyama, R.; Tanigaki, K. *J. Phys. Chem. Solids* **2007**, *69*, 1206.
(4) Biris, A. R.; Lupu, D.; Dervishi, E.; Li, Z.; Saini, V.; Saini, D.; Trigwell, S.; Mazumder, M. K.; Sharma, R.; Biris, A. S. *Part. Sci. Technol.* **2008**, *26*, 297.
(5) Naofumi, A.; Akasaka, T.; Watari, F.; Yokoyama, A. *Dent. Mater.* **2007**, *26*, 178.
(6) Stokes, P.; Khondaker, S. I. *Nanotechnology* **2008**, *19*, 175202.
(7) Kim, T.; Kim, S.; Olson, E.; Zuo, J. M. *Ultramicroscopy* **2008**, *108*, 613.
(8) Kong, J. A.; Cassell, A. M.; Dai, H. *Chem. Phys. Lett.* **1998**, *292*, 567.
(9) Nikolaev, P.; Bronikowski, M. J.; Bradley, R. K.; Rohmund, F.; Colbert, D. T.; Smith, K. A.; Smalley, R. E. *Chem. Phys. Lett.* **1999**, *313*, 91.
(10) Bachilo, S. M.; Balzano, L.; Herrera, J. E.; Pompeo, F.; Resasco, D. E.; Weisman, R. *J. Am. Chem. Soc.* **2003**, *125*, 11186.
(11) Iijima, S.; Ajayan, P. M.; Ichihashi, T. *Phys. Rev. Lett.* **1992**, *69*, 3100.
(12) Malesevic, A.; Vitchev, R.; Schouteden, K.; Volodin, A.; Zhang, L.; Tendeloo, G. V.; Vanhulsel, A.; Haesendonck, C. V. *Nanotechnology* **2008**, *19*, 305604.
(13) Stankovich, S.; Dikin, D. A.; Dommett, G. H. B.; Kohlhass, K. M.; Zimney, Z. J.; Stach, E. A.; Piner, R. D.; Nguyen, S. T.; Rouff, R. S. *Nature* **2006**, *442*, 282.
(14) Geim, A. K.; MacDonald, A. H. *Phys. Today* **2007**, *60*, 35.
(15) Novoselov, K. S.; Jiang, Z.; Zhang, Y.; Morozov, S. V.; Stormer, H. L.; Zeitler, U.; Maan, J. C.; Boebinger, G. S.; Kim, P.; Geim, A. K. *Science* **2007**, *315*, 1379.
(16) Wang, X.; Linjie, Z.; Mullen, K. *Nano Lett.* **2008**, *8*, 323.

Published on Web 10/20/2009

low-cost method will expand its scope in various applications.

One of the first successful methods to produce both single-layer and few-layer graphene was micromechanical exfoliation of bulk graphite.[19−22] However, this method is difficult to control and, hence, is not suitable for mass production. In other studies, large quantities of graphene nanosheets were produced via a soft chemical synthesis route and an ultrahigh-vacuum CVD route on different substrates.[23−25] Nevertheless, note that these methods are time-consuming and their yields are typically low, which limits their abilities to have significant economic and technological impact. Recently, promising techniques of large-scale graphene that are solution based and solvothermal-based have been demonstrated.[26,27]

In this manuscript, we report a novel approach for the large scale production of CNTs and graphene nanosheets on a single catalyst system using radio-frequency catalytic chemical vapor deposition (RF-cCVD). This is a well-known technique that has been used previously for high-quality carbon nanotube synthesis and is a very attractive synthesis routine for many reasons.[28,29] The RF-cCVD method significantly reduces the energy consumption during synthesis while preventing the formation of amorphous carbon and other types of unwanted byproduct. Furthermore, this method has been shown to improve the yield and crystallinity of CNTs.[29]

Although many monometallic catalysts have been successfully used to grow different types of CNTs, bimetallic alloys formed by transition metals generally provide greater nanotube efficiency.[30] As compared with Fe or Co monometallic catalysts under identical reaction parameters, the bimetallic Fe−Co/MgO catalyst systems were observed to provide a higher CNT growth yield when acetylene or methane was utilized as a carbon source.[31] Furthermore, we have previously reported that CNTs with the highest yield and crystallinity were obtained on the Fe−Co/MgO catalyst system with a stoichiometric composition of 2.5:2.5:95 (wt %).[31] This is the primary reason why, for this work, the Fe−Co/MgO (2.5:2.5:95 (wt %)) catalyst system was chosen over many other such systems. A porous MgO oxide was selected as the support because it can be removed by a relatively mild acid such as HCl, while other supports such as alumina and silica require a highly toxic treatment for their removal.[32]

For the first time, to our best knowledge, we report the synthesis of different types of carbon nanostructures such as CNTs and graphene nanosheets on the same catalytic system by varying only the reaction temperature. Being able to perform large-scale synthesis of different types of CNTs (single-wall carbon nanotubes (SWNTs), double-wall carbon nanotubes (DWNTs), and multi-wall carbon nanotubes (MWNTs)), as well as few-layer graphene sheets, using the same production technique and only altering one reaction parameter, significantly reduces the production costs for these materials.

Experimental Details

The Fe−Co/MgO catalyst system with a stoichiometric composition of 2.5:2.5:95 (wt %), was prepared via the impregnation method.[31] First, the weighted amounts of metal salts, $Fe(NO_3)_3 \cdot 9H_2O$ and $Co(NO_3)_2 \cdot 6H_2O$, were dissolved separately in ethanol with agitation. Next, MgO with a surface area of 130 m^2/ g was completely dispersed into 30 mL of ethanol and the metal salt mixtures were added to this solution. The final mixture was sonicated for ~1 h. Next, the ethanol was evaporated under continuous agitation, and the catalyst system was further dried overnight at 60 °C. Finally, the catalyst was calcinated in air at 500 °C for 2 h.

CNTs and graphene nanosheets were synthesized via RF-cCVD on the MgO supported Fe−Co bimetallic catalyst system utilizing acetylene as a hydrocarbon source. Approximately 100 mg of the catalyst was uniformly spread into a thin layer on a graphite susceptor and placed in the center of a quartz tube with an inner diameter of 1 in. The tube was purged with argon (the carrier gas) for 10 min at 150 mL/min. Next, the RF generator, which provides a very fast heating rate of 300−350 °C/min, was powered on and used to heat the graphite boat to the desired synthesis temperature. The temperature of the susceptor was permanently monitored with an optical pyrometer and was determined to be very uniform. At this point, acetylene was introduced at 4.5 mL/min for 30 min. The synthesis temperature was varied over a range of 700−1000 °C at 50° C increments and the final products were characterized after each reaction. At the end of each synthesis, the system was cooled under the presence of argon for 10 min. The as-produced carbon nanostructures were purified in one step by washing with a diluted HCl solution under sonication.

To determine the intrinsic weight loss of the catalyst, a "blank" experiment without the hydrocarbon source and only with argon was performed. The efficiency or the yield (η, expressed as a percentage) of the carbonaceous products that

(17) Berger, C.; Song, Z. M.; Li, X. B.; Wu, X. S.; Brown, N.; Nand, C.; Mayon, D.; Li, T. B.; Hass, J.; Marchenkov, A. N.; Conrad, E. H.; First, P. N.; de Heer, W. A. *Science* **2006**, *312*, 1191.
(18) Geim, A. K.; Novoselov, K. S. *Nat. Mat.* **2007**, *6*, 183.
(19) Novoselov, K. S.; Geim, A. K.; Morozov, S. V.; Jiang, D.; Katsnelson, M. I.; Grigorieva, I. V.; Dubonos, S. V.; Firsov, A. A. *Nature* **2005**, *438*, 197.
(20) Hummers, W. S.; Offeman, J. R. E. *J. Am. Chem. Soc.* **1958**, *80*, 1339.
(21) Hao, R.; Qian, W.; Zhang, L.; Hou, Y. *Chem. Commun.* **2008**, *48*, 6576.
(22) Li, X.; Wang, X.; Zhang, L.; Lee, S.; Dai, H. *Science* **2008**, *319*, 1229.
(23) Wang, G.; Yang, J.; Park, J.; Gou, X.; Wang, B.; Liu, H.; Yao, J. *J. Phys. Chem.* **2008**, *112*, 8192.
(24) Sutter, P. W.; Flege, J. I.; Sutter, E. A. *Nat. Mat.* **2008**, *7*, 406.
(25) Stancovich, S.; Dikin, D. A.; Piner, R. D.; Kohlhass, K. A.; Kleinhammes, A.; Jia, Y.; Wu, Y.; Nguyen, S. T.; Rouff, R. S. *Carbon* **2007**, *45*, 1558.
(26) Tung, V. C.; Allen, M. J.; Yang, Y.; Kaner, R. B. *Nat. Nanotechnol.* **2009**, *4*, 25.
(27) Choucair, M.; Thordarson, P.; Stride, J. A. *Nat. Nanotechnol.* **2009**, *4*, 30.
(28) Dervishi, E.; Li, Z.; Biris, A. R.; Lupu, D.; Trigwell, S.; Biris, A. S. *Chem. Mater.* **2007**, *19*, 179.
(29) Biris, A. R.; Biris, A. S.; Lupu, D.; Trigwell, S.; Dervishi, E.; Rahman, Z.; Marginean, P. *Chem. Phys. Lett.* **2006**, *429*, 204.
(30) Flahaut, E.; Govindaraj, A.; Peigney, A.; Laurent, C.; Rousset, A.; Rao, C. N. R. *Chem. Phys. Lett.* **1999**, *300*, 236.
(31) Dervishi, E.; Li, Z.; Xu, Y.; Saini, Y.; Watanabe, F.; Biris, A. S.; Bonpain, A.; Garbay, J. J.; Meriet, A.; Richard, M. *Part. Sci. Technol.* **2008**, *27*, 222.
(32) Ago, H.; Imamura, S.; Okazaki, T.; Saito, T.; Yumura, M.; Tsuji, M. *J. Phys. Chem. B* **2005**, *109*, 10035.

resulted after each synthesis was calculated according to the following formula:

$$\eta\,(\%) = \left[\frac{m_{ar} - m_b}{m_{br}}\right] \times 100 \qquad (1)$$

where m_{ar} is the mass of the sample after the synthesis, m_{br} the mass of the catalyst before the reaction, and m_b the mass of the catalyst after the blank experiment.

Characterization Techniques. To characterize the morphological properties of CNTs and graphene nanosheets, several techniques such as the microscopy, Raman scattering spectroscopy, and X-ray diffraction (XRD) were utilized.

Transmission electron microscopy (TEM) images were collected on a JEOL Model JEM-2100F field-emission TEM system that was equipped with a charge-coupled device (CCD) camera. The acceleration voltage was 100 kV for the graphene analysis. The carbon nanostructures were homogeneously dispersed in 2-propanol under ultrasonication for 30 min. Next, a few drops of the suspension were deposited on the TEM grid, dried, and evacuated before analysis. Scanning electron microscopy (SEM) images were obtained using a JEOL Model 7000F high-resolution scanning electron microscope. This microscope has a resolution of 1.2 nm at an accelerating voltage of 15 kV and a working distance of 10 mm. The final products were mounted on aluminum pins with double-sided carbon tape, and their corresponding SEM images were obtained.

Scanning tunneling microscopy (STM) images were obtained from a home-built beetle-style STM system with a RHK Technology Model SPM1000 controller and XMP software with an Axon Model CV4 current amplifier. STM imaging was performed in dry N_2 at room temperature. A drop of graphene solution (flakes of graphene dispersed in isopropanol) was deposited on a gold/mica substrate and allowed to dry in air. Atomic force microscopy (AFM) measurements were performed using a Veeco Model Dimension 3100 instrument with a scan range of 90 μm for the x/y-direction and 6 μm for the z-direction. After the graphene sheets were individually dispersed into 2-propanol solution, a few drops of the final solution were pipetted onto silicon substrates. Next, the substrates were air-dried and placed directly under the AFM tip for morphology analysis.

Raman scattering spectra were recorded at room temperature using Horiba Jobin Yvon Model LabRam HR800 system that was equipped with a CCD and a spectrometer with a grating of 600 lines/mm. A He-Ne laser (633 nm) was used as an excitation source. The laser beam intensity measured at the sample was kept at 5 mW and Raman shifts were calibrated with a silicon wafer at a peak of 521 cm^{-1}. The powder XRD profiles of the graphene sheets were recorded in the $\theta-2\theta$ mode on the Bruker D8 Discovery diffraction system (Bruker AXS Corporation). The monochromatic Cu Kα radiation line and general area detector diffraction system were used as an excitation source and detector, respectively. The experiments were conducted in Bragg−Brentano geometry. Quantitative analysis was performed with whole pattern fitting and Rietveld refinement.

Results and Discussions

1. Different Nanostructures Grown at Various Temperatures. Figure 1a shows a schematic diagram of the growth process for the high-quality carbon nanostructures using the RF generator. As the reaction temperature was varied over a range of 700−1000 °C, CNTs or

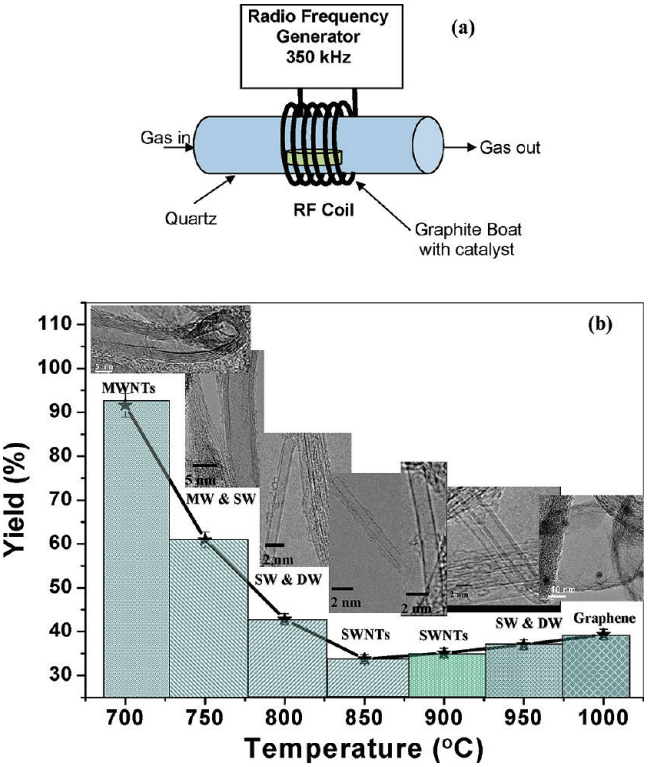

Figure 1. (a) Schematic diagram of the growth process for the carbon nanostructures using the RF generator. (b) Yield and TEM images of the CNTs and graphene produced through pyrolysis of acetylene under radio frequency heating as the reaction temperature was varied over a range of 700−1000 °C.

graphene nanosheets were synthesized by RF-cCVD technique on the MgO-supported Fe−Co bimetallic catalyst system, utilizing acetylene as a hydrocarbon source. Figure 1b shows the efficiencies of the carbon nanostructures synthesized at different reaction temperatures, as calculated using eq 1. The nanotubes grown at 700 °C were determined to have the highest yield of 91.6%, while those grown at 850 °C presented the lowest efficiency at ∼33.7%. To better understand the influence of the reaction temperature on the growth of different nanostructures, their morphological properties were characterized by TEM analysis after each synthesis. Crystalline MWNTs synthesized at 700 °C had ∼10−15 walls and their inner diameters varied over a range of 4−6 nm.

A small amount of SWNTs (∼10%) with diameters of ∼2 nm were observed at 750 °C, in addition to MWNTs. A large amount of bundled SWNTs, as well as a small amount of DWNTs (∼20%) with inner diameters of 2 nm, were synthesized at 800 °C. SWNTs with average diameters of 1.5 and 2 nm were synthesized at 850 and 900 °C, respectively. Furthermore, the efficiency results correlate well with the TEM images of the different nanostructures. As shown in Figure 1b, the finalized products synthesized at 800 and 950 °C, which contain SWNTs and DWNTs, have slightly higher yields, compared to SWNTs grown at 850 and 900 °C. Clearly, the carbon content efficiency is dependent on the nanotube wall number, where CNTs with the largest number of walls show the highest synthesis yield. SWNTs showed the lowest yield whereas the DWNTs were produced

with slightly higher efficiencies and MWNTs were observed to have the highest yield. The surprisingly observed change from SWNTs and DWNTs to SWNTs and back again to SWNTs and DWNTs, as the temperature was increased from 800 °C to 950 °C, could be explained by the magnetic phase transitions in the carbon itself, which affects the way C atoms condensate on the catalyst system.[33] As represented in Figure 1b, a large amount of graphene nanosheets were synthesized when the reaction temperature was increased to 1000 °C. Therefore, when acetylene is utilized as a hydrocarbon source, different types of nanotubes as well as graphene nanosheets may be synthesized on the same catalytic system, depending on the synthesis temperature.

Generally, MWNTs are synthesized at low temperatures (600−750 °C), whereas SWNT growth occurs at higher reaction temperatures (800−1200 °C), depending on the type of hydrocarbon utilized.[34,35] This indicates that SWNTs have a higher energy of formation, most probably because of their small diameters, resulting in high curvature and high strain energy.[36] It was determined that the diameter distributions of CNTs, as well as the number of their graphitic walls and their degree of graphitization, are strongly dependent on the size of the active metal nanoparticles present in the support.[37] Usually, small catalyst nanoparticles have a higher reactivity than larger ones and, hence, a catalyst system containing metal nanoparticles with very small dimensions in the range of 1−2.5 nm yields SWNT growth with small diameters.[38] The activation energies for processes of hydrocarbon diffusion and carbon nanostructure nucleation may be greater for small catalyst nanoparticles relative to bigger ones.[33] It was also shown that larger metal nanoclusters yielded DWNTs, as well as few-walled nanotubes with large diameters.[39,40]

The reaction temperature has a tremendous effect on the morphological properties of the catalytic system and, hence, on the CNT growth.[40,41] The solubility of the C atoms in the metal nanoparticles is controlled by the particle size of the transition metals and the synthesis temperature.[42] A mixture between SWNTs and DWNTs synthesized at 800 and 950 °C may be due to the presence of Fe/Co metal nanoparticles with a wide diameter distribution. This variation in size distribution could be explained by thermally activated phenomena such as surface diffusion or Ostwald ripening.[43] As the reaction temperature varies over a range of 700−1000 °C, the active metal nanoparticles have a tendency to split into finer particles or agglomerate into larger ones due to surface diffusion, hence yielding nanotube growth with various wall numbers. This change in catalyst morphology may help explain the versatility of the Fe−Co/MgO catalyst system, which yields different types of CNTs, depending on the reaction temperature. The temperature effects on the catalyst system could also be due to the magnetic phase changes in the catalyst and carbon itself. In 2001, Little demonstrated that, as the temperature increases, the magnetic moment of the catalyst system diminishes, which could explain the change from MWNT to SWNT growth that is observed in this work.[33] Higher temperature softens the catalyst system, changing the big particles to smaller metal nanoparticles and slowing the hydrocarbon decomposition, absorption, diffusion and carbon condensation for less MWNTs and more DWNTs or SWNTs.[44] The reason for the growth of graphene nanosheets at 1000 °C is not yet fully understood. We believe that the high reaction temperature plays an important role not only on the catalyst system but also in the decomposition of the hydrocarbon.[29] At 1000 °C, the catalyst nanoparticles melt completely, generating a better wetting property, which is more suitable for the formation of the graphene structure.[44] Other investigators have experimentally and computationally demonstrated magnetic metal atoms cutting graphene and unzipping CNTs.[45,46] Furthermore, Zhao et al. reported ferromagnetic transitions of carbon at temperatures of 900−1000 °C, which may be responsible for the synthesis of the different types of carbon nanostructures demonstrated in this manuscript.[47]

Hence, these particular reaction parameters were determined to be optimal for graphene synthesis. Further work in our laboratory is focused on understanding this mechanism better. Therefore, fine-tuning the synthesis temperature is very crucial in the synthesis of CNTs or graphene nanosheets when acetylene is utilized as the carbon source.

Raman spectroscopy was used to analyze the crystallinity and the diameter distribution of the nanotubes. Figure 2a shows the representative Raman scattering spectra with all the vibrational modes (RBM, D band, G band, and 2D band) of the carbon nanostructures synthesized at different temperatures. The intensities of D and G bands were measured to analyze the quality of CNTs grown under different conditions. As shown in Figure 2b, the CNTs grown at 850 °C were determined to have the highest G/D ratio, whereas those grown at 700 °C showed the lowest G/D ratio. These findings

(33) Little, R. B. U.S. Patent 6,761,871, **2001**.
(34) Charlier, J. C.; Iijima, S. *Top. Appl. Phys.* **2001**, *80*, 55.
(35) Dai, H. *Top. Appl. Phys.* **2001**, *80*, 29.
(36) Karthikeyan, S.; Mahalingam, P.; Karthik, M. *E-J. Chem.* **2009**, *6*, 1.
(37) Saito, T.; Ohshima, S.; Xu, W.; Ago, H.; Yumura, M.; Iijima, S. *J. Phys. Chem. B* **2005**, *109*, 10647.
(38) Yamada, T.; Namai, T.; Hata, K.; Futaba, D. N.; Mizuno, K.; Fan, J.; Yudasaka, M.; Yumura, M.; Iijima, S. *Nat. Nanotechnol.* **2006**, *1*, 131.
(39) Ago, H.; Nakamura, K.; Imamura, S.; Tsuji, M. *Chem. Phys. Lett.* **2004**, *391*, 308.
(40) Dervishi, E.; Li, Z.; Watanabe, F.; Xu, Y.; Saini, V.; Biris, A. R.; Biris, A. S. *J. Mater. Chem.* **2009**, *19*, 3004.
(41) Zhang, Y.; Li, Y.; Kim, W.; Wang, D.; Dai, H. *Appl. Phys. A: Mater. Sci. Process.* **2002**, *74*, 325.
(42) Rummeli, M. H.; Kramberger, C.; Loffler, M.; Jost, O.; Bystrzejewski, M.; Gruneis, A.; Gemming, T.; Pompe, W.; Buchner, B.; Pichler, T. J. *Phys. Chem. B* **2007**, *111*, 8234.
(43) Feng, D.; Arne, R.; Kim, B. *Carbon* **2005**, *43*, 2215.
(44) Little, R. B. *J. Cluster Sci.* **2003**, *14*(2), 135.
(45) Boukhvalov, D. W.; Katsnelson, M. I. *Appl. Phys. Lett.* **2009**, *95*, 023109.
(46) Ci, L.; Song, L.; Jariwala, D.; Laura Elías, A.; Gao, W.; Terrones, M.; Ajayan, P. M. *Adv. Mater.* **2009**, *21*, 1.
(47) Zhao, G. M.; Beeli, P. *Phys. Rev. B* **2008**, *77*, 245433.

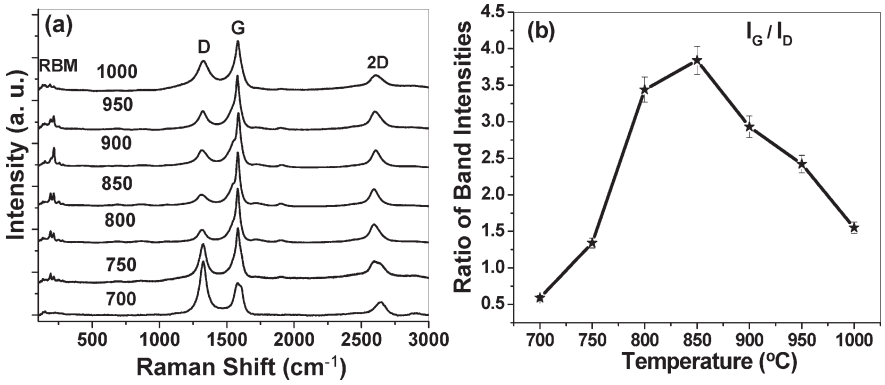

Figure 2. (a) Representative Raman spectra of the carbon nanostructures synthesized with acetylene at different temperatures; (b) the G/D intensity ratio versus reaction temperature.

correlate well with the TEM results, which showed that highly crystalline MWNTs were synthesized at 700 °C and high-yield SWNTs were synthesized at 850 °C. It is well-known that the G/D ratio decreases as the number of the nanotube walls increases. The Raman spectrum of graphene is discussed in more detail in the next section.

The RBM regions of the Raman spectra for each of the products were thoroughly studied to determine their diameter distributions. The RBM peaks are usually observed within the range of 100−500 cm^{-1}, and their positions are strongly dependent on the diameter and chirality of the nanotubes.[48,49] Often, the TEM images reveal that most of the nanotubes are bundled, which affects their RBM peak positions when compared to isolated CNTs. Theoretical calculations of SWNTs have shown that tube diameter (d) and the radial mode frequency (ω_{RBM}) exhibit the following straightforward relationship:

$$\omega_{RBM}\ (cm^{-1}) = \frac{\alpha}{d\ (nm)} + a \qquad (2)$$

where $\alpha = 234\ cm^{-1}\cdot nm$ and $a = 10$, depending on the excitation energy and bundle sizes.[49,50] This equation takes into account van der Waal interactions between the SWNTs when they are bundled in ropes.[51]

The RBM regions of the corresponding Raman spectra for the CNTs synthesized between 800 and 950 °C were thoroughly studied to determine their diameter distributions. Both SWNTs and DWNTs revealed RBM features, with each peak corresponding to a particular diameter of the graphitic tubes.[49] These nanoscale phenomena are not present in the Raman scattering spectra of the MWNTs, which contain larger nanotube diameters and wider diameter distribution.[48] The RBM region is absent in the Raman spectra of the MWNTs that were mostly synthesized at 700 and 750 °C and of the graphene sheets grown at 1000 °C. Table 1 summarizes the RBM peaks and their corresponding diameters calculated using eq 2 for the SWNTs and DWNTs synthesized in the temperature range of 800−950 °C. The corresponding nanotube diameters varied between 2.22 nm and 0.86 nm. The RBM peaks at 190 and 213 cm^{-1}, which correspond to diameters of 1.15 and 1.3 nm, respectively, are present in all of the samples. Furthermore, the SWNTs synthesized at 900 °C had a very sharp RBM peak at 215 cm^{-1}, which corresponds to a diameter of 1.14 nm. These findings correlate well with the TEM images, revealing that these SWNTs have a very narrow diameter distribution.

Table 1. Spectral Position and the Corresponding Diameter Values of the RBM Peaks Collected with a 633-nm Laser Excitation for the Carbon Nanotubes (CNTs) Grown with Acetylene over a Temperature Range of 800−950 °C

CNT_acetylene, λ_{exc} = 633 nm	
ω_{RBM} (cm^{-1})	d (nm)
115	2.22
131	1.93
132	1.91
145	1.73
148	1.69
190	1.3
193	1.27
212	1.158
213	1.152
215	1.141
250	0.975
252	0.966
256	0.951
279	0.869
280	0.866
282	0.86

2. Graphene Analysis. High-quality few-layer graphene sheets (between 1 and ~5 layers) were successfully synthesized on the same Fe−Co/MgO (2.5:2.5:95 wt %) catalytic system at 1000 °C. The synthesized graphene sheets were fully analyzed by several microscopy techniques. TEM analysis revealed a high yield production of few-layer graphene structures. High- and low-resolution TEM images (see Figure 3a and its inset) revealed that the as-produced samples are composed of graphene sheets overlaid side by side, with dimensions varying over a range of 100−110 nm in diameter. They were determined to be very stable under the electron beam.

(48) Dresselhaus, M. S.; Dresselhaus, G.; Saito, R.; Jorio, A. *Phys. Rep.* **2005**, *409*, 47.
(49) Rao, A. M.; Chen, J.; Richter, E.; Schlecht, U.; Eklund, P. C.; Haddon, R. C.; Venkateswaran, U. D.; Kwon, Y. K.; Tománek, D. *Phys. Rev. Lett.* **2001**, *86*, 3895.
(50) Strong, K. L.; Anderson, D. P.; Lafdi, K.; Kuhn, J. N. *Carbon* **2003**, *41*, 1477.
(51) Kuzmany, H.; Plank, W.; Hulman, M.; Kramberger, C.; Gruñeis, A.; Pichler, T. *Eur. Phys. J. B* **2001**, *22*, 307.

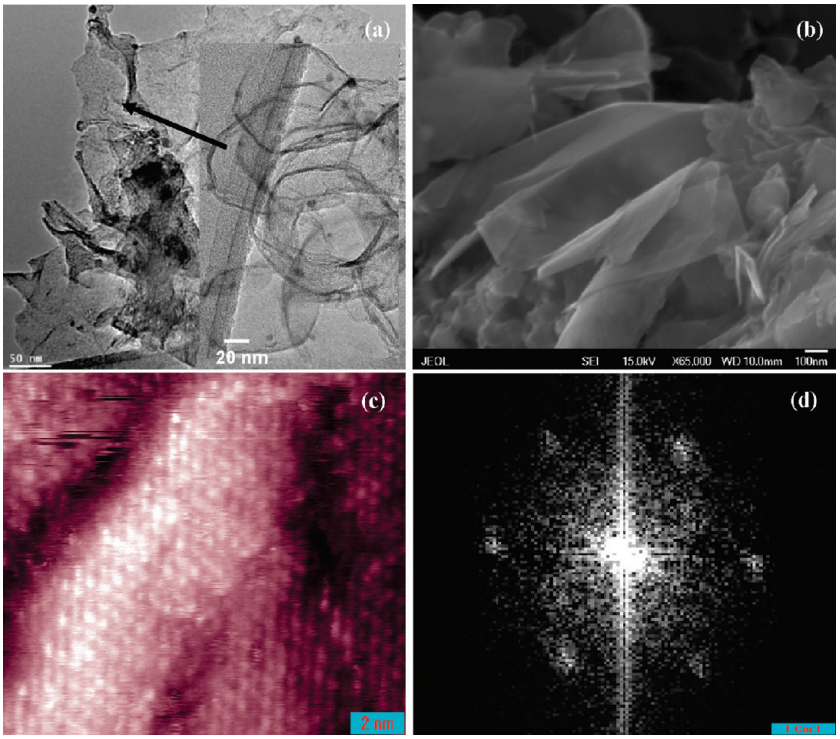

Figure 3. (a) Low-magnification TEM image of the graphene nanosheets deposited on top of the carbon coated copper grid. The inset shows a high resolution image of the few-layer graphene sheets with diameters of ~100 nm. (b) SEM image of the semitransparent graphene sheets synthesized in large quantities. (c) STM image of the molecular structure of graphene layers on a gold/mica substrate, obtained at a bias of 1 V with a tunneling current of 1.27 pA. Scan area for the image is 20 nm × 20 nm. (d) Fourier transform image showing the hexagonal structure of the graphene layers.

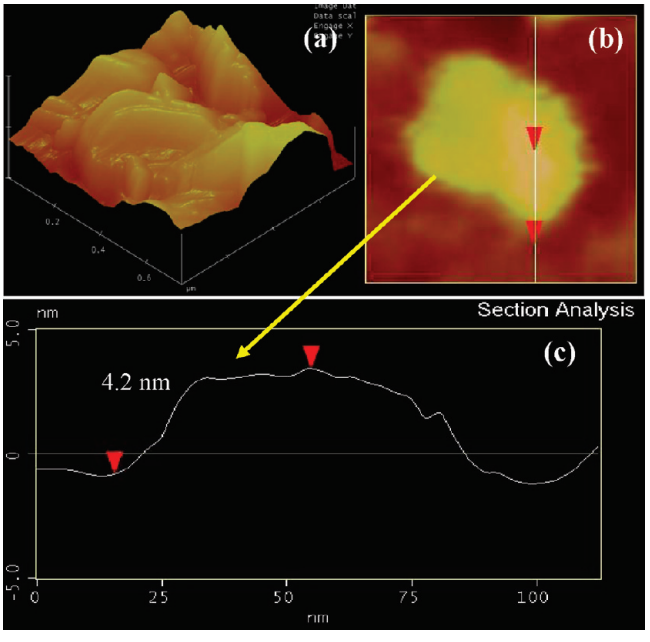

Figure 4. (a) Three-dimensional (3D) representation of a 1 μm × 1 μm AFM scan of graphene sheets overlaid onto a silicon surface; (b) AFM image of the few-layer graphene sheets, with a corresponding height image shown in panel (c).

The SEM images revealed that most of the graphene sheets are semitransparent, indicating that they have very few layers. The data obtained from TEM and SEM analysis were also determined to be in good correlation with the results obtained through STM. Figure 3c shows a STM topographic image of few-layer graphene sheets. In bulk graphite, the C atoms on the surface are not equivalent. This results in an asymmetry of the surface atom electronic environment that produces a 3-fold symmetry pattern. Our fast Fourier transform (FFT) analysis (see Figure 3d) is consistent with the 3-fold symmetry pattern. The dark regions in the image correspond to vacancy islands that represent one-atomic-layer-deep pits in the Au{111} surface; this is a characteristic that is due to growth conditions.[52]

Figures 4a and 4b show the AFM images of the few-layer graphene deposited onto a silicon wafer. The structure of these nanomaterials observed in the AFM images is similar to that observed in the TEM analysis. AFM was also utilized to measure the thickness of the synthesized graphene nanosheets. The AFM height image shown in Figure 3c indicates that the thickness of the graphene sheets is 3−5 nm, corresponding to ~3−5 layers.

Raman spectroscopy is a nondestructive technique that has been successfully used to characterize the crystallinity and the number of layers of graphene.[53,54] The typical Raman spectra of few layer graphene have three main peaks, which are commonly referenced as the D band (~1350 cm^{-1}), the G band (~1580 cm^{-1}), and the 2D band (~2650 cm^{-1}). The D band arises due to the

(52) Vericat, C.; Vela, M. E.; Salvarezza, R. C. *Phys. Chem. Chem. Phys.* **2005**, *7*, 3258.
(53) Ferrari, A. C.; Meyer, J. C.; Scardaci, V.; Casiraghi, C.; Lazzeri, M.; Mauri, F.; Piscanec, S.; Jiang, D.; Novoselov, K. S.; Roth, S.; Geim, A. K. *Phys. Rev. Lett.* **2007**, *97*, 189401.
(54) Graf, D.; Molitor, F.; Ensslin, K.; Stampfer, C.; Jungen, A.; Hierold, C.; Wirtz, L. *Nano Lett.* **2007**, *7*, 238–242.

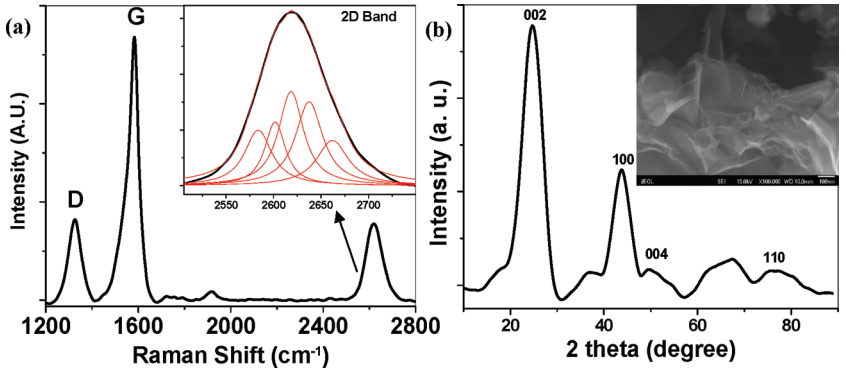

Figure 5. (a) Raman spectrum of the few-layer graphene samples collected with 633-nm laser excitation at 20 mW; the inset shows the curve-fitted 2D band with five Lorentzian curves. (b) XRD pattern of the few-layer graphene sheets showing several distinct diffraction peaks; the inset shows the SEM image of crystalline graphene sheets (scale bar = 100 nm).

breathing modes of sp^2 atoms in rings and its intensity is usually associated with defects in the carbon-based material.[55] The G band, which is characteristically due to the bond stretching of sp^2 atoms in both ring and chains, is often called the E_{2g} mode at the Brillouin zone center.[56,57] The 2D band is the second order of the D band, and its shape, as well as its position, is used to identify a single-layer sheet from bilayer and few-layer (< 5 layers) graphene sheets.[16]

Figure 5a shows the Raman spectrum of graphene grown via our method and measured at a laser excitation of 633 nm (20 mW). Although the intensity of the D band is associated with defects, in the case of graphene, it was observed that a substantial contribution comes from edge effects.[57] Therefore, we hypothesize that the presence of the D band shown in this Raman spectrum arises mostly because of the edges and steps present in the graphene samples. The intense G and 2D peaks present near 1583 and 2620 cm^{-1} are characteristic of the few-layer graphene sheets, as previously reported.[27,58] Furthermore, the full width at half-maximum (fwhm) of the 2D peak was used to determine the number of layers present in the exfoliated graphene.[52] Analyzing the Raman spectrum and using the relationship fwhm(2D) = $[-45(1/N) + 88]$ cm^{-1}, where N is the number of layers, it was calculated that the graphene presented in this work contains ~3−5 layers.[59] In addition, the 2D band can be decomposed into five components (Lorentzian peaks), which is a characteristic feature of the Raman spectra of few-layers (< 5 layers) graphene, as previously reported.[52,57] The inset of Figure 5a shows the Raman spectrum near the 2D peak curve fitted with five Lorentzian peaks.

XRD was used to analyze the crystallinity and estimate the number of layers in the graphene nanosheets. Figure 5b shows the XRD profile of graphene sheets grown via the RF-cCVD method. The intense peak positions at C(002) and C(100), which are typical features for graphite, are identified in this graphene XRD pattern.[60] In addition, the peaks at 24.8° (002) and 50.1° (004) are characteristic of the parallel graphene layers, whereas the 43.7° (100) and 76.7° (110) diffraction peaks correspond to the 2D in-plane symmetry along the graphene sheets.[60] The peak position of the C(002) was used to calculate the layer-to-layer distance, which is also known as the d-spacing, between two subsequent graphene sheets.[12] The crystallite size was evaluated from the width of the diffraction peaks using the Scherrer equation (K = 0.9).[61] Using the values of the d-spacing and the crystallite size, the graphene sheets were determined to have, on average, 3−5 layers. These results are in good agreement with the Raman spectroscopy analysis. The inset in Figure 5b shows the SEM image of the as-produced semitransparent graphene nanosheets.

Conclusions

Different types of nanostructures including nanotubes and graphene nanosheets were synthesized on the same Fe−Co/MgO catalytic system by utilizing the radio-frequency catalytic chemical vapor deposition (RF-cCVD) method. The product efficiencies were dependent on the morphological properties of the nanostructures and varied with temperature. When acetylene was utilized as the hydrocarbon source, variations in synthesis temperature (in the range of 700−1000 °C) lead to single-wall nanotube (SWNT), double-wall nanotube (DWNT), multi-wall nanotube (MWNT), or graphene synthesis. Highly crystalline MWNTs were mostly grown at 700 and 750 °C, whereas large quantities of few-layer graphene sheets (1−5 layers) were synthesized at 1000 °C. As revealed by the TEM analysis, SWNTs as well as DWNTs were synthesized when the temperature was varied over a range of 800−950 °C. The graphene samples were thoroughly characterized by microscopy, spectroscopy, and X-ray diffraction techniques. The findings from all the different techniques indicated the presence of highly

(55) Ferrari, A. C. *Solid State Commun.* **2007**, *143*, 47.
(56) Das, A.; Chakraborty, B.; Sood, A. K. *Bull. Mater. Sci.* **2008**, *31*, 579.
(57) Reina, A.; Jia, X.; Ho, J.; Nezich, D.; Son, H.; Bulovic, V.; Dresselhaus, M. S.; Kong *Nano Lett.* **2009**, *9*, 30.
(58) Graf, D.; Molitor, F.; Ensslin, K.; Stampfer, C.; Jungen, A.; Hierold, C.; Wirtz, L. *Solid State Commun.* **2007**, *143*, 44.
(59) Lee, D. S.; Riedl, C.; Krauss, B.; von Klitzing, K.; Starke, U.; Smet, J. H. *Nano Lett.* **2008**, *8*, 4320.
(60) Dimovski, S.; Nikitin, A.; Ye, H.; Gogotsi, Y. *J. Mater. Chem.* **2004**, *14*, 238.
(61) Biscoe, J.; Warren, B. *J. Appl. Phys.* **1942**, *12*, 346.

crystalline and few-layer graphene sheets with diameters in the range of 100−110 nm. It was determined that the synthesis temperature has a strong influence on the reaction yield, as well as on the type of the nanostructures synthesized with acetylene. Finally, a low-cost production of various nanostructures including graphene and carbon nanotubes (CNTs) in large quantities can be attained using a highly versatile Fe−Co/MgO (2.5:2.5:95 wt %) catalytic system and only varying one reaction parameter.

Acknowledgment. This research was partially supported by the U.S. Department of Energy (DOE) (Grant No. DE-FG 36-06 GO 86072). The financial support from Arkansas Science and Technology Authority (ASTA), through Grant No. 08-CAT-03, is highly appreciated.